Supplemental Fig. 1

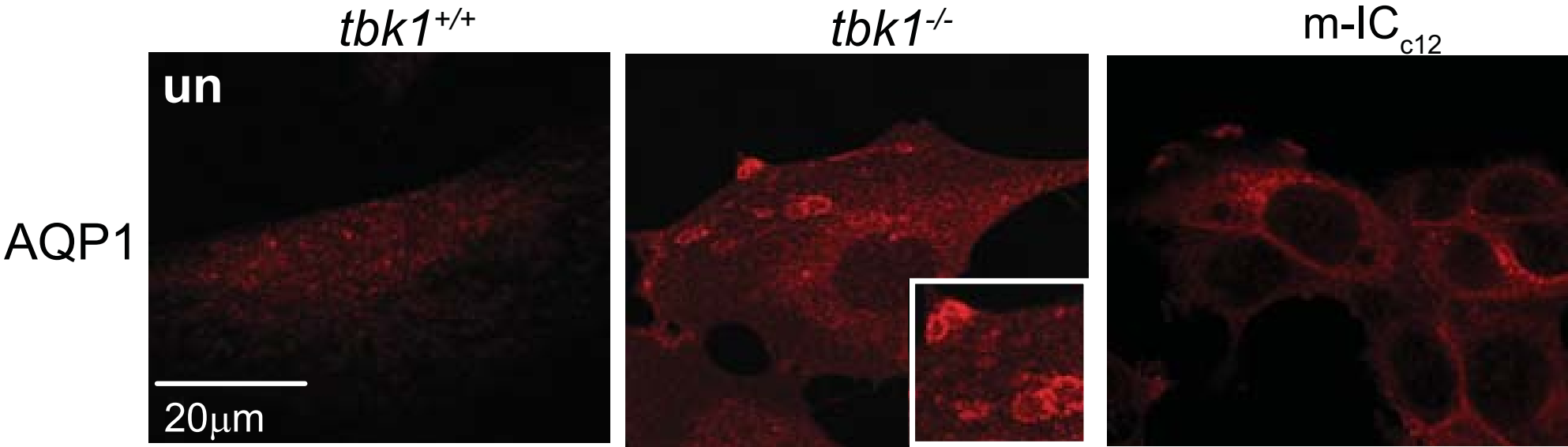

Supplemental Fig. 2

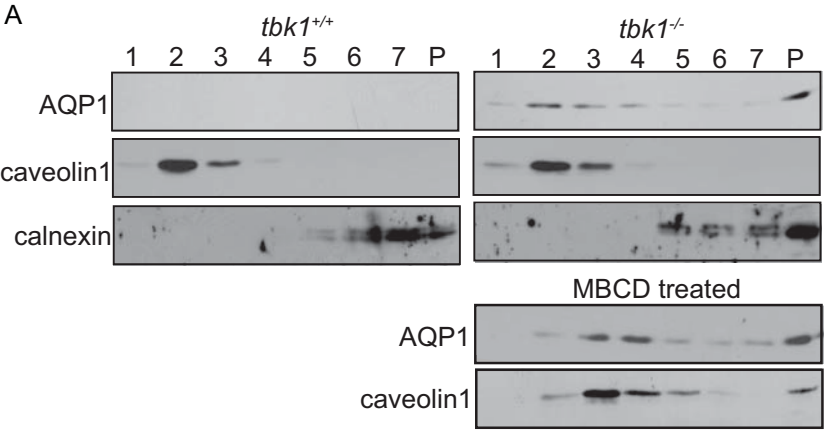

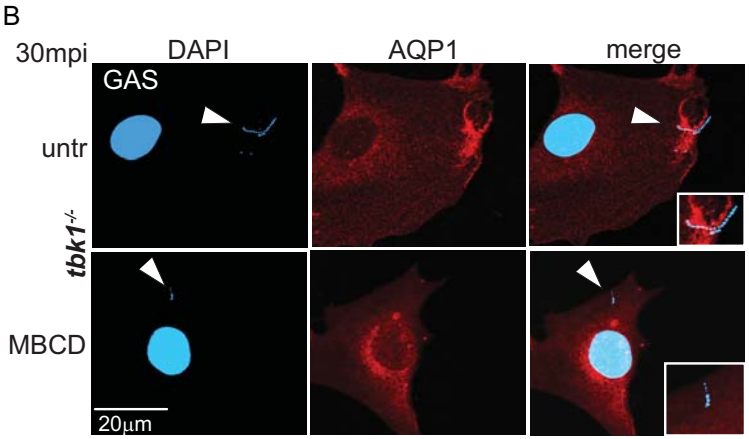

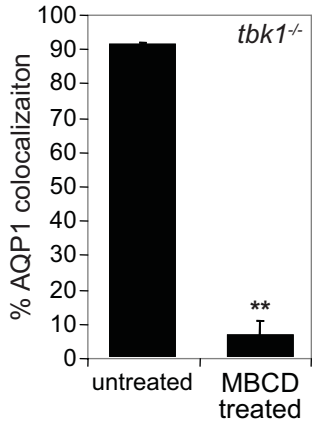

Supplemental Fig. 3

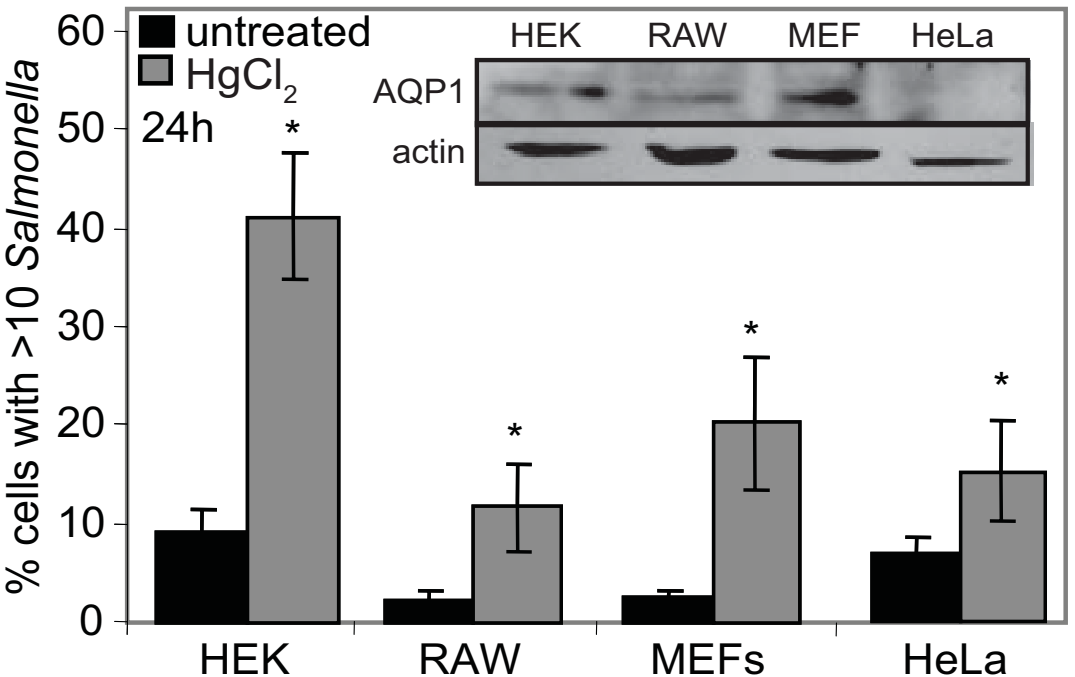

Supplemental Data

Figure Legends

Fig. S1. Subcellular localization of AQP1 in uninfected cells. A. Confocal immunofluorescence microscopy of uninfected *tbk1*$^{+/+}$ MEFs, *tbk1*$^{-/-}$ MEFS, and m-IC$_{c12}$ stained with anti-AQP1 antibody.

Fig. S2. PCV can acquire AQP1 upon pathogen entry at cholesterol rich microdomains (CRM).

A. Immunoblot analysis of non-detergent based isolation CRM from *tbk1*$^{+/+}$ and *tbk1*$^{-/-}$ MEFs. Numbers represent sequential fractions taken from a discontinuous sucrose gradient containing cell lysate; 1-top fraction, P-pellet. CRM located in fractions 1-3, non-CRM fractions located in fractions 4-7, and the pellet contains whole cells. The immunoblots were probed for AQP1, caveolin-1; control for CRM localized proteins, and calnexin; control for non-CRM protein localization. *Tbk1*$^{-/-}$ MEFs were treated for 1hr with MBCD to deplete cholesterol and probed with anti-AQP1 and anti-caveolin-1 antibody.

B. Confocal immunofluorescence microscopy of *tbk1*$^{-/-}$ MEFs untreated or treated with MBCD for 1hr to deplete membrane cholesterol, washed, and replaced with medium without FBS. Cells were infected for 1h pi with GAS (arrowheads) and stained with anti-AQP1 antibody and DAPI to visualize bacteria.

C. *Tbk1*$^{-/-}$ MEFs treated as in (B); percentages represent # of GAS that colocalized with AQP1/100 bacteria from 3 independent experiments (** p<0.001).

Fig. S3. Dysregulated AQP1 function leads to loss of PCV integrity. MEFs, HeLa, HEK, and RAW264.7 cells were left untreated or treated with $HgCl_2$ and infected with *Salmonella* and fixed at 24h pi. Percentages reflect # cells with >10 *Salmonella*/100

cells (n=3); mean of triplicates ± SD is shown. * indicate $p < 0.05$ comparing treated to untreated cells for each cell type. Insert: Immunoblot of AQP1 expression in cells using anti-AQP1 antibody. Blots were loaded with ~3 times more protein than in Fig. 1C to permit visualization of AQP1, and re-probed with anti-actin antibody as a loading control.

Movie S1.

Live-cell imaging of *tbk1*$^{-/-}$ MEFs infected with GAS (phase dark chains) for 30 min in medium containing 70kDa Texas Red-dextran to label intact vacuoles (red). Frames were taken every 2 min for 2hrs.

Supplemental Materials and Experimental Procedures

Reagents and strains

Antibodies against various antigens were obtained from the following sources: AQP1 (AB3065; Chemicon International), Calnexin (SPA-860; Stressgen Bioreagents Corp.), Caveolin-1 (610406; BD Transduction Laboratories), actin (sc-1615; Sigma-Aldrich). 4',6-Diamidino-2 phenylindole dihydrochloride (DAPI) was purchased from BioChemika, and 70,000 MW fluorescent Texas-Red dextran was purchased from Invitrogen. Where indicated, MEFs were pretreated with 10μM $HgCl_2$ (Sigma-Aldrich) for 1h and throughout experiment. Methyl-β-cyclodextrin (MBCD) (Sigma-Aldrich) was used at 7.5mM in medium without FBS. After 1h, cells were washed twice and medium without FBS was replaced.

The *Salmonella enterica* serovar Typhimurium strain used was wildtype SL1344 expressing green fluorescent protein (GFP). The Group A Streptococcus (GAS) strain used was GAS188 (Hakansson *et al.*, 2005, Sierig *et al.*, 2003).

Cell culture and infections

Tbk1$^{+/+}$ and *tbk1*$^{-/-}$ MEFs (G. Barber, University of Miami) were immortalized by continuous culture and clonally derived as previously described (Radtke *et al.*, 2007). MEFs cells were grown in RPMI medium supplemented with 10% fetal bovine serum and 1% L-glutamine at 37°C in 5% CO_2. Bacterial strains and HeLa and RAW264.7 cells (American Type Culture Collection) were derived and cultured as previously described (Radtke *et al.*, 2007). HEK cells were a kind gift from Dr. H. Mobley, and were infected similarly to MEFs at an moi of 10.

Microscopy

Confocal immunofluorescence analysis was performed as previously reported (Radtke *et al.*, 2007). To determine % cells with >10 *Salmonella*, cells were infected with *Salmonella,* fixed at 24h pi, and the number of viable host cells (with normal nuclear morphology as observed by DAPI staining) containing > 10 *Salmonella* per 100 infected cells was counted in at least 3 independent experiments. Colocalization of GAS with AQP1 was determined by fixing cells at 30m pi, staining the cells with anti-AQP1 antibody and DAPI, than counting the number of bacteria colocalized with AQP1 per 100 in 3 independent experiments. Live cell imaging was performed by infecting MEFs on a coverslip with medium containing GAS and 5mg/ml TR-dextran for 30 min. The cells were washed, and Ringer's Buffer with 100μg/ml gentamicin was added to the coverslip in a live-cell imaging chamber. Cells were visualized on an Olympus IX70 inverted microscope, and frames were taken every 2 min for at total of 2hr. The frames were analyzed and made into movies using Metamorph Premier software (Universal Imaging Corporation).

Isolation of vacuoles and cholesterol rich microdomains

Uninfected and *Salmonella* containing vacuoles was performed with modifications as described; in brief, $1.2x10^7$ MEF cells were either harvested or infected with *Salmonella* for 0.5h and then harvested and resuspended in cold homogenization buffer (Anes *et al.*, 2003). The cells were lysed using a 22-gauge needle; nuclei and intact cells were removed by centrifugation at 500xg for 5 minutes. The supernatant was layered on top of a discontinuous sucrose gradient of 60%, 40%, and 25% sucrose, which was centrifuged at 100,000xg for 60 minutes at 4°C. For isolation of CRM, MEFs were infected with *Salmonella* at an moi of 50 for 1h, followed by purification of CRM fractions using a non-detergent based method of discontinuous gradient centrifugation (Vetrivel *et al.*, 2004, Waugh *et al.*, 1999).

Statistical analysis

Data sets in triplicate were compared using Student's unpaired *t*-test for independent samples. P-values of <0.05 (*) and <0.001 (**) were considered significant and highly significant respectively.

References

Anes, E., Kuhnel, M.P., Bos, E., Moniz-Pereira, J., Habermann, A. and Griffiths, G. (2003). Selected lipids activate phagosome actin assembly and maturation resulting in killing of pathogenic mycobacteria. *Nat Cell Biol* **5,** 793-802.

Hakansson, A., Bentley, C.C., Shakhnovic, E.A. and Wessels, M.R. (2005). Cytolysin-dependent evasion of lysosomal killing. *Proc. Natl. Acad. Sci. U. S. A.* **102,** 5192-5197.

Radtke, A.L., Delbridge, L.M., Balachandran, S., Barber, G.N. and O'Riordan M, X. (2007). TBK1 protects vacuolar integrity during intracellular bacterial infection. *PLoS Pathog* **3,** e29.

Sierig, G., Cywes, C., Wessels, M.R. and Ashbaugh, C.D. (2003). Cytotoxic effects of Streptolysin O and Streptolysin S enhance the virulence of poorly encapsulated Group A Streptococci. *Infect. Immun.* **71,** 446-455.

Vetrivel, K.S., Cheng, H., Lin, W., Sakurai, T., Li, T., Nukina, N.*, et al.* (2004). Association of gamma-secretase with lipid rafts in post-Golgi and endosome membranes. *J. Biol. Chem.* **279,** 44945-44954.

Waugh, M.G., Lawson, D. and Hsuan, J.J. (1999). Epidermal growth factor receptor activation is localized within low-buoyant density, non-caveolar membrane domains. *Biochem. J.* **337 (Pt 3),** 591-597.

Supplemental Table 1

gene	primer sequence
qRT-PCR	
actin	F-5’ AGGTGTGATGGTGGGAATGG
	R-5‘ GCCTCGTCACCCACATAGGA
aqp1	F-5’ AATGCTACAGCTTGTGTTGCAGCC
	R-5‘ ACCTGAAGAATGTGGCTCTCGGTT
cloning	
aqp1	F-5’ GGGGTACCGGAGTTGAGCACCAGGCATCCAGCG
	R-5’ GAATTCCGTTGGGCCAATGCAGAGAGAAGACT